

## Supplementary Information

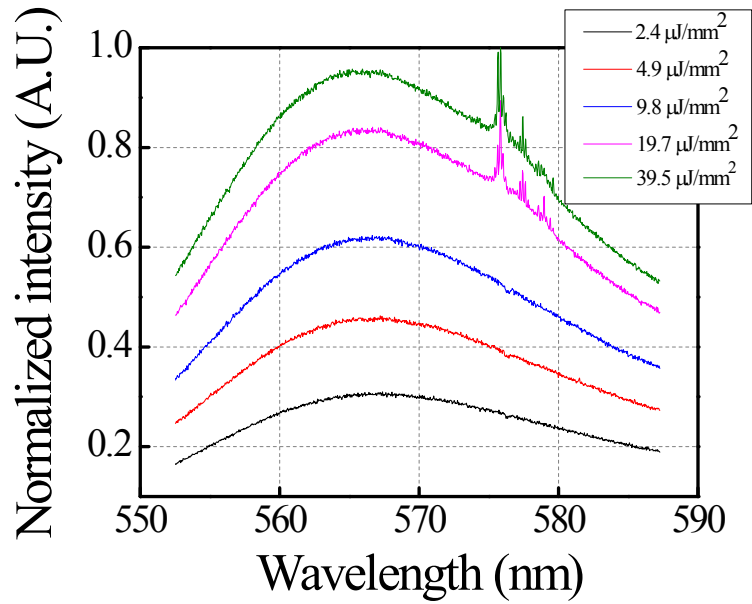
### **Monolithic Optofluidic Ring Resonator Lasers Created by Femtosecond Laser Nanofabrication**

Hengky Chandralim<sup>1</sup>, Qiushu Chen<sup>1</sup>, Ali A. Said<sup>2</sup>, Mark Dugan<sup>2</sup>, and Xudong Fan<sup>1\*</sup>

<sup>1</sup>Department of Biomedical Engineering, University of Michigan,  
Ann Arbor, MI 48109, USA

<sup>2</sup>Translume Inc., 655 Phoenix Drive, Ann Arbor, MI, USA

\*[xsfan@umich.edu](mailto:xsfan@umich.edu)



**Supplementary Figure 1:** Emission spectra as a function of pump fluence below and just above the lasing threshold. A 1200 g/mm grating was used to achieve wider spectral coverage. For comparison purposes, all emission spectra are normalized to the highest peak value. High resolution (0.05 nm) spectra using a 2400 g/mm grating are plotted in Fig. 4(A).

**Table 1: Parameters used in the present work**

Parameters	Definitions	Units
$\lambda_p$	Pump wavelength	nm
$\lambda_L$	Lasing wavelength	nm
$\lambda_E$	Fluorescence peak wavelength	nm
$n_{Sol}$	Refractive index of Solvent	-
$n_T$	Rhodamine 6G (R6G) dye concentration	$cm^{-3}$
$n_X$	Dye concentration at excited state	$cm^{-3}$
$\sigma_a(\lambda_p)$	Absorption cross-section at $\lambda_p$	$cm^2$
$\sigma_a(\lambda_L)$	Absorption cross-section at $\lambda_L$	$cm^2$
$\sigma_e(\lambda_L)$	Emission cross-section at $\lambda_L$	$cm^2$
$E(\lambda)$	Fluorescence quantum distribution	$nm^{-1}$
$q$	Quantum yield of RG6 in quinoline	-
$q_{Ref}$	Quantum yield of RHB in ethanol	-
FL-Slope <sub>Sol</sub>	Fluorescence efficiency of RG6 in quinoline	$nM^{-1}$
FL-Slope <sub>Ref</sub>	Fluorescence efficiency of RHB in ethanol	$nM^{-1}$
$\sigma$	Standard deviation of RG6 fluorescence distribution	ns
$\epsilon_{Sol}$	Extinction coefficient of RG6	$M^{-1}cm^{-1}$
$\epsilon_{Ref}$	Extinction coefficient of RHB	$M^{-1}cm^{-1}$
$\tau_F$	Fluorescence lifetime	ns
A	$\sigma_A(\lambda_L)/\sigma_A(\lambda_p)$	-
B	$\sigma_A(\lambda_L)/\sigma_E(\lambda_L)$	-
C	$Q_{Dye}/\eta Q_0$	-
h	Planck constant	Js
c	Speed of light in vacuum	m/s
$\Delta t$	Pulse width of the pump laser	ns
$\eta$	Light coupling efficiency	-
$P_{th}$	Lasing photon density threshold	#photons/ $m^2$
$\Phi_{th}$	Lasing fluence threshold	$\mu J/mm^2$
$Q_{Dye}$	Q-factor due to dye absorption	-
$Q_{Sol}$	Q-factor due to solvent absorption	-
$Q_{Rad}$	Q-factor due to radiation loss	-
$Q_{Sc}$	Q-factor due to scattering loss	-
$Q_0$	Q-factor of the laser cavity in the absence of gain medium	-

### Q-factor analysis

Based on the lasing theory and the experimentally measured lasing threshold, the cavity Q-factor in the absence of the gain medium (*i.e.*,  $Q_0$ ) can be calculated. The lasing threshold is given by:

$$n_X \sigma_E(\lambda_L) = (n_T - n_X) \sigma_a(\lambda_L) + \frac{2\pi n_{Sol}}{\lambda_L \eta Q_0} \quad (S1)$$

Equation (S1) can be written as:

$$\gamma \equiv \frac{n_X}{n_T} = \frac{\sigma_a(\lambda_L)}{\sigma_e(\lambda_L) + \sigma_a(\lambda_L)} \cdot \left(1 + \frac{Q_{Dye}}{\eta Q_0}\right) \quad (S2)$$

The stimulated emission cross section is obtained from the following expression:

$$\sigma_e(\lambda_L) = \frac{\lambda_L^4 E(\lambda_L)}{8\pi c n_{Sol}^2 \tau_F} \quad (S3)$$

According to the four energy level model, at steady state,  $\gamma$  relates to the dimensionless pump intensity by:

$$\gamma = \frac{I}{I+1}, \quad (S4)$$

$$\text{and } I = \frac{\gamma}{1-\gamma}, \quad (S5)$$

where  $I = P \cdot \sigma_a(\lambda_p) \cdot \tau_F$ .  $P$  is the power density in units of (# of photons per  $m^2$  per second).

Equations (S2) and (S5) can be combined:

$$\frac{P_{th}}{\Delta t} \cdot \sigma_a(\lambda_p) \cdot \tau_F = \frac{\frac{\sigma_a(\lambda_L)}{\sigma_e(\lambda_L) + \sigma_a(\lambda_L)} \cdot [1+C]}{1 - \frac{\sigma_a(\lambda_L)}{\sigma_e(\lambda_L) + \sigma_a(\lambda_L)} \cdot [1+C]} = \frac{1}{\sigma_e(\lambda_L)} \frac{\sigma_a(\lambda_L) \cdot [1+C]}{1 - \frac{\sigma_a(\lambda_L)}{\sigma_e(\lambda_L)} \cdot C} \quad (S6)$$

$P_{th}$  can be expressed in a simpler form as:

$$P_{th} = \frac{\Delta t}{\sigma_e(\lambda_L) \cdot \tau_F} A \frac{1+C}{1-B \cdot C} \quad (S7)$$

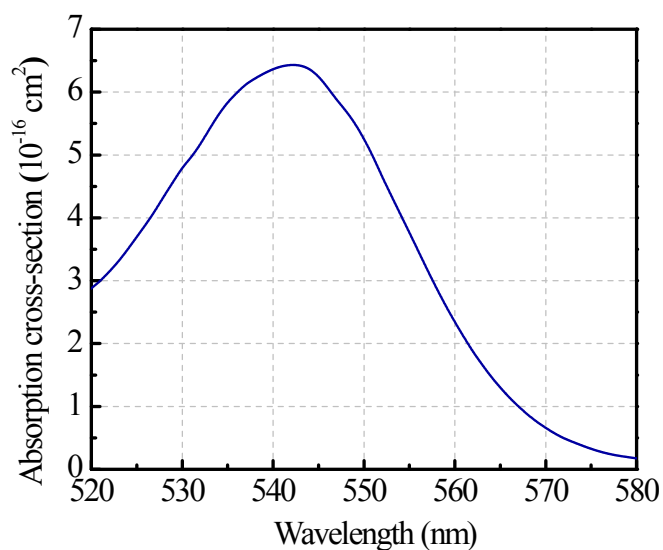
where  $A = \frac{\sigma_a(\lambda_L)}{\sigma_a(\lambda_p)}$ ,  $B = \frac{\sigma_a(\lambda_L)}{\sigma_e(\lambda_L)}$ , and  $C = \frac{Q_{Dye}}{\eta Q_0}$ .

$Q_{Dye}$  can be calculated by:

$$Q_{Dye} = \frac{2\pi n_{Sol}}{\lambda_L n_T \sigma_a(\lambda_L)} \quad (S8)$$

$P_{th}$  is related to the excitation fluence at the pump wavelength by:

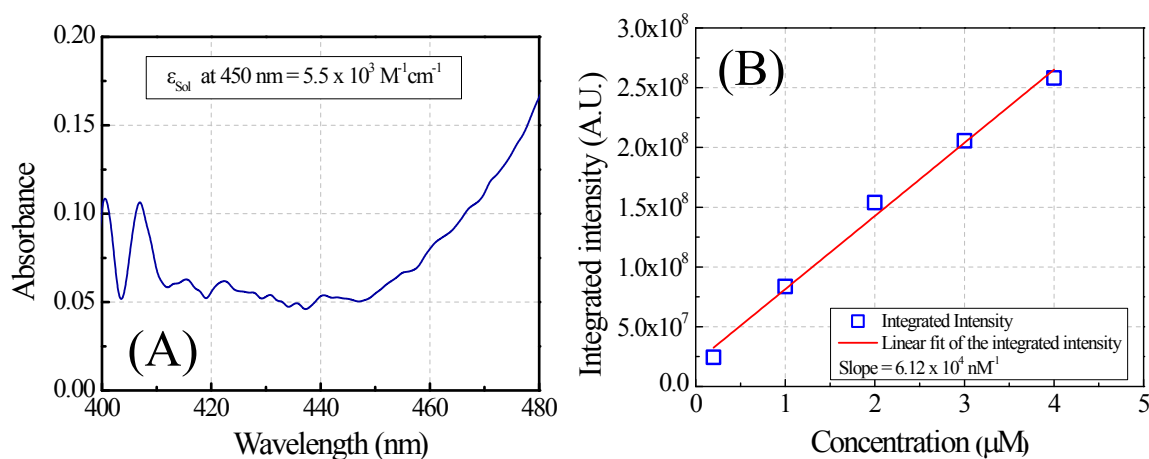
$$\Phi_{th} = P_{th} \cdot \frac{h \cdot c}{\lambda_p} = \frac{h \cdot c \cdot \Delta t}{\sigma_e(\lambda_L) \cdot \lambda_p \cdot \tau_F} A \frac{1+C}{1-B \cdot C} \quad (S9)$$



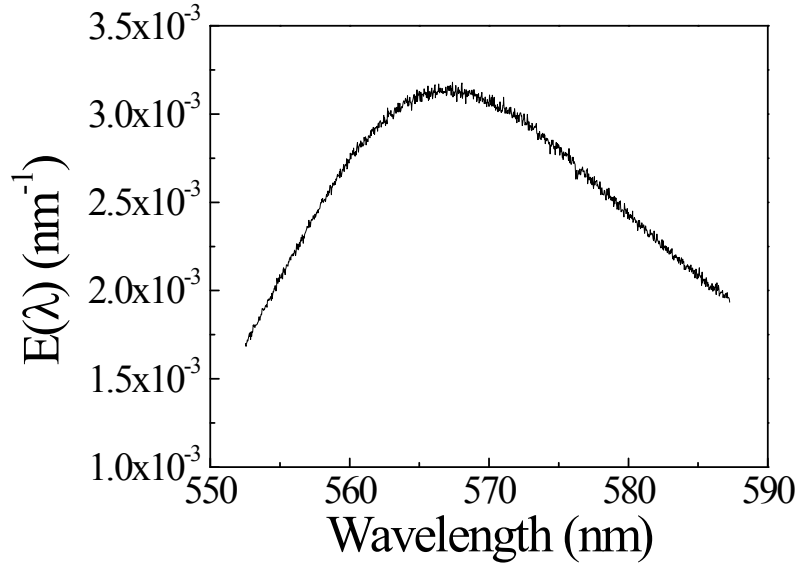
**Supplementary Figure 2:** Absorption cross-section of RG6 in quinoline based on absorbance measurement with 10  $\mu\text{M}$  solution.

In order to acquire necessary parameters to analyze  $Q_0$  in equation (S9), we performed several measurements and data extractions. We measured the Rhodamine 6G (R6G) dye absorption cross-section as presented in Fig. S2 and obtained  $\sigma_a(\lambda_P)$  and  $\sigma_a(\lambda_L)$ .  $Q_{\text{Dye}}$  was calculated to be  $9.07 \times 10^3$  according to equation (S8).

Next, we need to determine the fluorescence quantum distribution  $E(\lambda)$  and fluorescence lifetime ( $\tau_F$ ) of the RG6 in quinoline to calculate  $\sigma_e(\lambda_L)$  in equation (S3). In order to compute  $E(\lambda)$ , we need to first calculate the quantum yield ( $q$ ) and measure the fluorescence spectrum of the dye solution. To determine the quantum yield, we performed absorption and fluorescence measurements of RG6 dye in quinoline and compared the results against a reference dye solution (Rhodamine B (RhB) in ethanol) which has a known  $q_{\text{Ref}}$  value<sup>1</sup>. Fluorescence test was done with FluoroMax-4



**Supplementary Figure 3:** (A) Absorbance of RG6 dye in quinoline as a function of wavelength. (B) Integrated fluorescence intensity as a function of RG6 dye concentration.



**Supplementary Figure 4:** Fluorescence quantum distribution,  $E(\lambda)$ .

spectrofluorometer (Horiba Scientific). Absorption test was performed with NanoDrop 2000c spectrophotometer (Thermal Scientific). The excitation wavelength for the absorption measurement was 450 nm. The measurement results shown in Fig. S3 indicate  $\epsilon_{Sol}$  and  $FL-Slope_{Sol}$  of  $5.5 \times 10^3 \text{ M}^{-1}\text{cm}^{-1}$  and  $6.12 \times 10^4 \text{ nM}^{-1}$ , respectively.

Using the equation:

$$q = q_{Ref} \times \frac{FL - Slope_{Sol}}{FL - Slope_{Ref}} \times \frac{n_{Sol}^2}{n_{Ref}^2} \times \frac{\epsilon_{Ref}}{\epsilon_{Sol}} \quad (S10)$$

the fluorescence quantum yield,  $q$ , of 0.12 was obtained.

RG6 fluorescence quantum distribution,  $E(\lambda)$ , can be obtained through the fluorescence spectrum in Fig. S1(B) by considering that

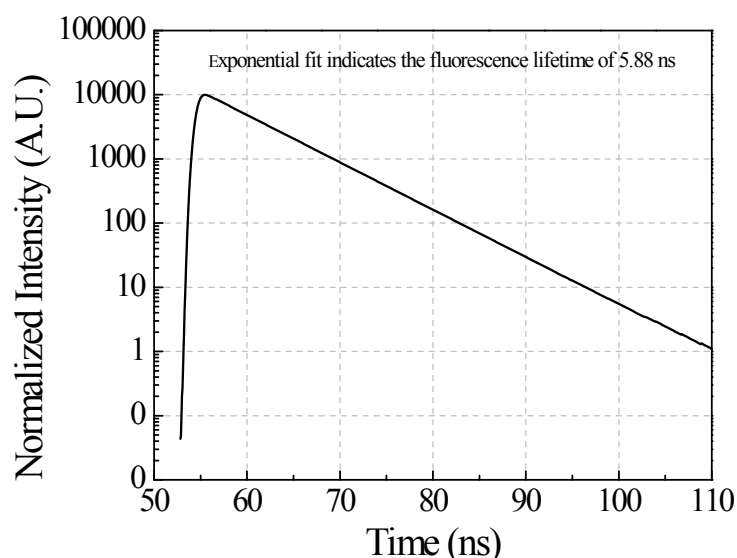
$$\int E(\lambda) \cdot d\lambda = q. \quad (S11)$$

According to Fig. S4

$$E(575 \text{ nm}) = 0.0028 \text{ nm}^{-1}. \quad (S12)$$

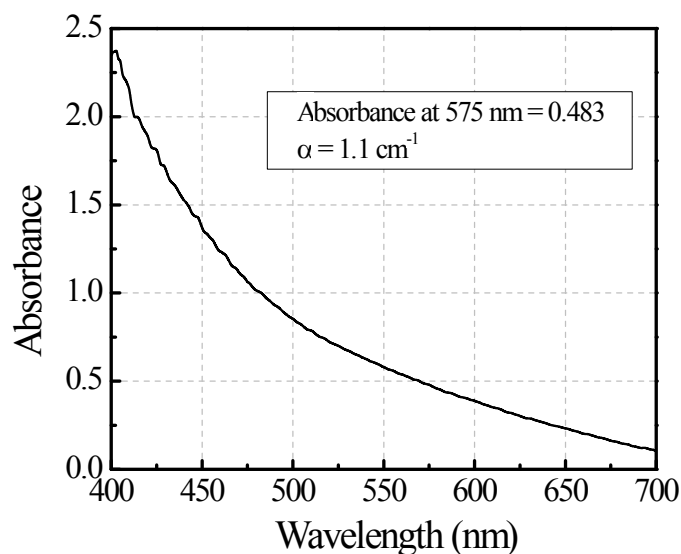
In the next step, we measured the fluorescence lifetime,  $\tau_F$  of the RG6 in quinoline. The measurement result of the time correlated photon counting experiment performed using a fluorescence lifetime spectrometer (TemPro, Horiba) is shown in Fig. S4. An exponential fit reveals 5.88 ns fluorescence lifetime of RG6 dye in quinoline. We substituted the measured parameters to equation (S3), and determined the stimulated emission cross-section,  $\sigma_e$ , of  $2.61 \times 10^{-17} \text{ cm}^2$ .

We have now all the parameters needed to extract  $Q_0$  from equation (S9). Considering an input pump fluence threshold ( $\Phi_{TH}$ ) of  $15 \mu\text{J}/\text{mm}^2$  during experiment, we calculate  $Q_0$  to be  $3.3 \times 10^4$ .



**Supplementary Figure 5:** Fluorescence decay curve obtained with 500  $\mu\text{M}$  RG6 dye in quinoline. The exponential fit reveals 5.88 ns fluorescence lifetime.

In order to validate the method used here to extract the Q-factor (*i.e.*,  $Q_0$ ), we employ the same theoretical model to estimate the lasing threshold of an optofluidic ring resonator laser reported in Ref. 2., which Q-factor is known (*i.e.*,  $\eta Q_0 = 4 \times 10^6$ ). Table 2 tabulates several key parameters used for this work and the work reported in reference<sup>2</sup>. Based on the parameters listed on the right column of Table 2, an estimated lasing fluence threshold of 22  $\text{nJ}/\text{mm}^2$  is obtained, very close to the experimentally measured result of 25  $\text{nJ}/\text{mm}^2$ . Therefore, our current approach to extract  $Q_0 = 3.3 \times 10^4$  using the lasing fluence threshold is justified.



**Supplementary Figure 6:** Absorbance measurement of quinoline as a function of wavelength.

**Table 2: Comparisons of the current work and the work in Ref. 2.**

<b>Parameters</b>	<b>Current work (1 mM R6G in quinoline)</b>	<b>Ref. 2 (2 mM R6G in ethanol)</b>
$\lambda_P$	532 nm	532 nm
$\lambda_L$	575 nm	600 nm
n	1.62	1.40
$n_T$	$6 \times 10^{17} \text{ cm}^{-3}$	$1.2 \times 10^{18} \text{ cm}^{-3}$
$\sigma_a(\lambda_P)$	$5.18 \times 10^{-16} \text{ cm}^2$	$2 \times 10^{-16} \text{ cm}^2$
$\sigma_a(\lambda_L)$	$3.25 \times 10^{-17} \text{ cm}^2$	$1 \times 10^{-19} \text{ cm}^2$
$\sigma_e(\lambda_L)$	$2.61 \times 10^{-17} \text{ cm}^2$	$1 \times 10^{-16} \text{ cm}^2$
$E(\lambda)$	$2.8 \times 10^{-3} \text{ nm}^{-1}$	$5.7 \times 10^{-3} \text{ nm}^{-1}$
q	0.12	0.9
$\tau_F$	5.88 ns	4.08 ns
A	$6.27 \times 10^{-2}$	$5 \times 10^{-2}$
B	1.25	$1 \times 10^{-3}$
C	0.28	0.3
$\Delta t$	5 ns	5 ns
$Q_{\text{Dye}}$	$9.07 \times 10^3$	$1.2 \times 10^6$
$\eta Q_0$	$3.3 \times 10^4$	$4 \times 10^6$
$\Phi_{\text{th}}$	$15 \mu\text{J}/\text{mm}^2$	$22 \text{ nJ}/\text{mm}^2$



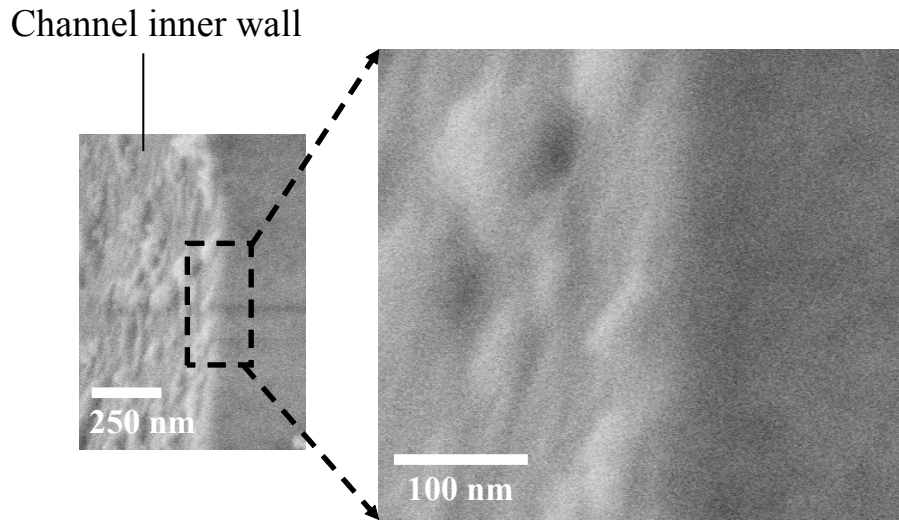
### Estimation of $Q_{Sc}$

The surface roughness of a pre-annealing device fabricated by the 3-D femtosecond laser writing process has previously been characterized to be 40-50 nm<sup>3</sup>. Fig. S6 shows the SEM image of the ring resonator inner wall taken after the ring resonator underwent thermal annealing. The roughness was reduced to approximately 30 nm.

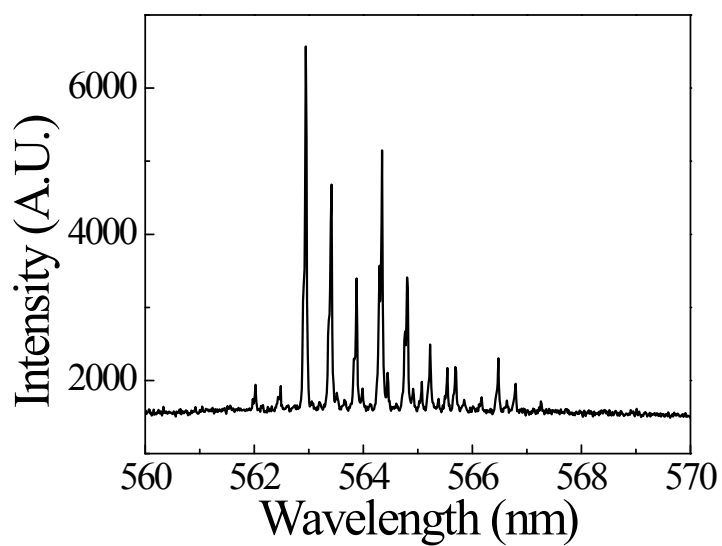
The roughness is related the Q-factor by<sup>4</sup>:

$$Q \propto \frac{1}{\sigma_{rough}^2 \cdot (n_{core}^2 - n_{cladding}^2)}, \quad (S13)$$

where  $\sigma_{rough}$  is the surface roughness.  $n_{core}$  and  $n_{cladding}$  are the refractive index for the ring and the cladding, respectively. Previous work on polymer ring resonators, whose surface roughness and the Q-factor have been well characterized and directly measured, provides a means to estimate the scattering loss related Q-factor of our ring resonator. According to Ref. 4,5, a Q-factor of  $5 \times 10^5$  was obtained at 780 nm for a polymer ring resonator with the surface roughness of 5-10 nm. Based on equation S13, the scattering loss related Q-factor of our ring resonator should range between  $3.2 \times 10^4$  and  $1.3 \times 10^5$ , in agreement with the scattering related Q-factor estimation ( $Q_{Sc} = 4.2 \times 10^4$ ) that we extract based on the lasing threshold.



**Supplementary Figure 7:** SEM images of the channel inner wall. The surface roughness (rms) is about 30 nm.



**Supplementary Figure 8:** Lasing emission from 1 mM R6G in chlorobenzene ( $n=1.524$ ) at a pump fluence of  $90 \mu\text{J}/\text{mm}^2$ . Flow rate was  $3 \mu\text{L}/\text{min}$ .

## References

1. F. L. Arbeloa, P. R. Ojeda, and I. L. Arbeloa, "Fluorescence self-quenching of the molecular forms of Rhodamine B in aqueous and ethanolic solutions," *J. Lumin.* **44**, 105-112 (1989).
2. S. Lacey, I. M. White, Y. Sun, S. I. Shopova, J. M. Cupps, P. Zhang, and X. Fan, "Versatile opto-fluidic ring resonator lasers with ultra-low threshold," *Opt. Express* **15**, 15523-15530 (2007).
3. Y. Sikorski, C. Rablau, M. Dugan, A. A. Said, P. Bado, and L. G. Beholz, "Fabrication and characterization of microstructures with optical quality surfaces in fused silica glass using femtosecond laser pulses and chemical etching," *Appl. Opt.* **28**, 7519-7523 (2006).
4. C.-Y. Chao, and L. J. Guo, "Reduction of Surface Scattering Loss in Polymer Microrings Using Thermal-Reflow Technique," *IEEE Photon. Technol. Lett.* **16**, 1498-1500 (2004).
5. T. Ling, S.-L. Chen, and L. J. Guo, "High-sensitivity and wide-directivity ultrasound detection using high Q polymer microring resonators," *Appl. Phys. Lett.* **98**, 204103 (2011).